Wetlands
DOI 10.1007/s13157-014-0558-6

ORIGINAL RESEARCH

Assessing Mangrove Above-Ground Biomass and Structure using Terrestrial Laser Scanning: A Case Study in the Everglades National Park

Emanuelle A. Feliciano · Shimon Wdowinski · Matthew D. Potts

Received: 7 November 2013 / Accepted: 11 June 2014

Abstract Mangroves are among the ecosystems with the highest potential for carbon sequestration and storage. In these ecosystems and others above-ground biomass (AGB) is often used to estimate above-ground carbon content. We used a Leica-ScanStation-C10 Terrestrial Laser Scanner (TLS) to estimate the volume and AGB of 40 mangrove trees distributed in three different mangrove sites located along Shark River Slough (SRS), in the western Everglades National Park. To estimate the volumetric shape of mangroves, we modeled stems as tapered geometrical surfaces called frustums of paraboloids and prop roots (*Rhizophora mangle*) as toroids and cylinders. AGB was estimated by multiplying the TLS-derived volume by wood specific density. Our TLS method for the SRS sites resulted in AGB estimates in the range of: 3.9±0.4 to 31.3±3.4 kg per tree in the short mangrove (<5 m) site, 27.4±3.0 to 119.1±12.9 kg per tree in the intermediate (<13 m) site and 52.1±6.7 to 1756.5±189.7 kg per tree in the tall (13–23 m) mangrove site. Our quantitative results: (1) enabled us to develop site-specific allometric relationships for tree diameter and AGB and (2) suggested that TLS is a promising alternative to destructive sampling.

Electronic supplementary material The online version of this article (doi:10.1007/s13157-014-0558-6) contains supplementary material, which is available to authorized users.

E. A. Feliciano (✉) · S. Wdowinski
Division of Marine Geology and Geophysics, University of Miami - Rosenstiel School of Marine and Atmospheric Science, 4600 Rickenbacker Causeway, Miami, FL 33149, USA
e-mail: efeliciano@rsmas.miami.edu

M. D. Potts
Department of Environmental Science, Policy and Management, University of California, 130 Mulford Hall #3114, Berkeley, CA 94720, USA

Keywords Mangrove vegetation · LIDAR · Terrestrial laser scanning (TLS) · Stem volume · Above-ground biomass, Forest structure, Allometry

Introduction

Mangroves are among the ecosystems with the highest potential for carbon sequestration and storage (Donato et al. 2011; Alongi 2012). These coastal ecosystems link terrestrial and aquatic environments; harbor unique biodiversity; provide storm protection; sequester nutrients, sediments and carbon; and provide shoreline stabilization (Alongi 2002; Giri et al. 2011). Anthropogenic disturbances (e.g. aquaculture, agriculture and coastal projects), and global warming (sea level rise) are threatening mangrove forests and the ecosystem services they provide (Alongi 2002). Although mangroves are relatively simple in structure, they are variable in stature (dwarf up to tall) and play an important role as blue carbon storage systems (Mcleod et al. 2011). Of the ecosystem services they provide, carbon sequestration is among the most important. Thus, quantifying the carbon stock of these tropical and subtropical tidal forests is of upmost importance as they form a vital part of the carbon cycle and rank among the most productive ecosystems (Twilley et al. 1992; Jennerjahn and Ittekkot 2002) in the world. In this paper we take an important first step to quantify one of the main components of carbon stock, tree-level above-ground biomass (AGB) in a mangrove ecosystem by using a cutting edge ground-based remote sensing technology.

Carbon stock of an ecosystem is usually divided into two major reservoirs: AGB and below-ground biomass (BGB). Previous studies have found that mangroves have a high BGB to AGB ratio (Saenger 1982; Sánchez 2005) and that most of the biomass (up to 98 %) is located and stored below-ground (Donato et al. 2011). However, quantitative

Published online: 27 June 2014

estimations of BGB can be obtained for small areas and require significant resources and efforts. Thus, using ground-based, airborne and spaceborne remote sensing technologies for estimating AGB is very attractive and important, as AGB provides a lower bound of the total biomass stored in an ecosystem. Additionally, tree-based AGB estimates are relatively simple to transform into estimates of carbon content, by multiplying AGB by the carbon concentration (CC) of the wood. Generally, it is common and accepted to multiply by a CC that ranges between 45 % and 50 % (Schlesinger and Bernhardt, 2013). For mangroves, there are reported CC values ranging from 45.9 % and 47.1 % (Kauffman et al. 2011), which fall on the published range for AGB conversion into above-ground carbon.

To date, the majority of published studies estimating AGB have used allometric equations, which usually relate tree size, shape, volume or AGB to tree diameter. The theoretical basis of allometry assumes that one or more parts of an organism are directly proportional to the growth or size of other tree parts. (Komiyama et al. 2008). Several studies have used allometry to estimate the AGB of mangroves. Diameter at breast height (DBH) has been used as a predictive variable to estimate AGB (Imbert and Rollet 1989; Fromard et al. 1998). Crown area, number of prop roots and total tree height have been used as AGB predictors (Coronado-Molina et al. 2004). DBH and total tree height were excellent AGB predictors (R^2=0.92) in a study by Smith and Whelan (2006) . Finally, DBH and wood specific density (WSD) were used to develop generic mangrove allometric equations that predict AGB (Chave et al. 2005; Komiyama et al. 2005).

Drawbacks of the allometric approach include the need for intensive fieldwork and vegetation harvesting to create allometric equations as well as the use of usually only one predictor variable (DBH) since other parameters (e.g. tree height and crown area) often have 10–15 % field measurement errors (Fromard et al. 1998). Another drawback is the limited applicability of the derived equations to a certain forest site and specific species. However, frequently, equations derived from one mangrove forest site are applied to other sites without knowing site-specific structural characteristics. Some studies have suggested that species-specific allometric relationships can change between regions and site conditions (e.g., Smith and Whelan 2006). It is recommended to use site-specific allometry to predict AGB, as abiotic conditions might yield unique characteristics not captured in general allometric equations (Rivera-Monroy et al. 2013).

Due to the drawbacks of developing allometric equations to estimate AGB, new approaches for precise AGB estimations are needed. In this study, we use a state-of-the-art Light Detection and Ranging (LiDAR)-based Terrestrial Laser Scanner (TLS) to estimate AGB. In recent years, the usage of TLS has been increasing in forestry. The main advantage of a TLS survey is its ability to capture a 3-D image of the forest structure. Several studies have shown that TLS can measure vegetation parameters such as DBH (Hopkinson et al. 2004; Watt and Donoghue 2005), tree height (Hopkinson et al. 2004; Maas et al. 2008) leaf area index (LAI) (Clawges et al. 2007) and non-explicit parameters such as wood-to-total-tree area and leaf-to-total-tree area (Clawges et al. 2007), basal area (Tansey et al. 2009), stem density (Maas et al. 2008; Liang et al. 2012) and AGB in juvenile trees (Seidel et al. 2011). To date, no study using TLS for a forestry application has been conducted in a mangrove ecosystem.

One common method used to estimate stem AGB of trees is to acquire information on WSD and multiply it by its stem volume. Estimating volume is a challenging task due to the geometry of trees, which resemble tapered surfaces (Husch et al. 2002). Moreover, estimating mangrove tree volume is even more challenging as *Rhizophora mangle* individuals have prop roots. Several studies have reported that AGB allocation in *R. mangle* prop roots can constitute between 2–47 % of the total AGB, depending on the maturity of the forest (Lugo and Snedaker 1974; Gong and Ong 1990; Fromard et al. 1998; Ross et al. 2001; Coronado-Molina et al. 2004). The goal of our study was two-fold. The first was to use TLS to estimate the volume, AGB, and AGB allocation of various individuals of different mangrove species. The second goal was to compare and contrast these TLS-derived estimates to published estimates calculated using traditional allometric methods.

Study Area

Our study area was located within a large mangrove forest along the southwestern coast of South Florida. The forest lies within the boundaries of the Everglades National Park (ENP) (Fig. 1) and consists mainly of three mangrove species: *Rhizophora mangle* L. (Red mangrove), *Laguncularia racemosa* (L.) C.F. Gaertn (White mangrove), and *Avicennia germinans* (L.) L. (Black mangrove). Mangrove canopy height in the region can reach up to 23 m (Simard et al. 2006). The mangrove communities used in our study area have been extensively studied with substantial research focused on nutrient exchange, root dynamics, physiological responses and CO_2 fluxes (Rivera-Monroy et al. 2007; Barr et al. 2009; Castaneda-Moya et al. 2011).

Within the study area we selected three measurement sites that were located along a tidal channel of Shark River Slough (SRS). We selected these sites because they are part of the comprehensively researched Florida Coastal Everglades – Long Term Ecological Research Network (FCE-LTER). The sites differed in the stature of the mangrove community: short (<5 m) (SRS-4), intermediate (<13 m) (SRS-5) and tall (13–23 m) (SRS-6) (Fig. 1c–f). *R. mangle* dominates SRS-4 and SRS-5, whereas *R. mangle*, *L. racemosa* and *A. germinans* are

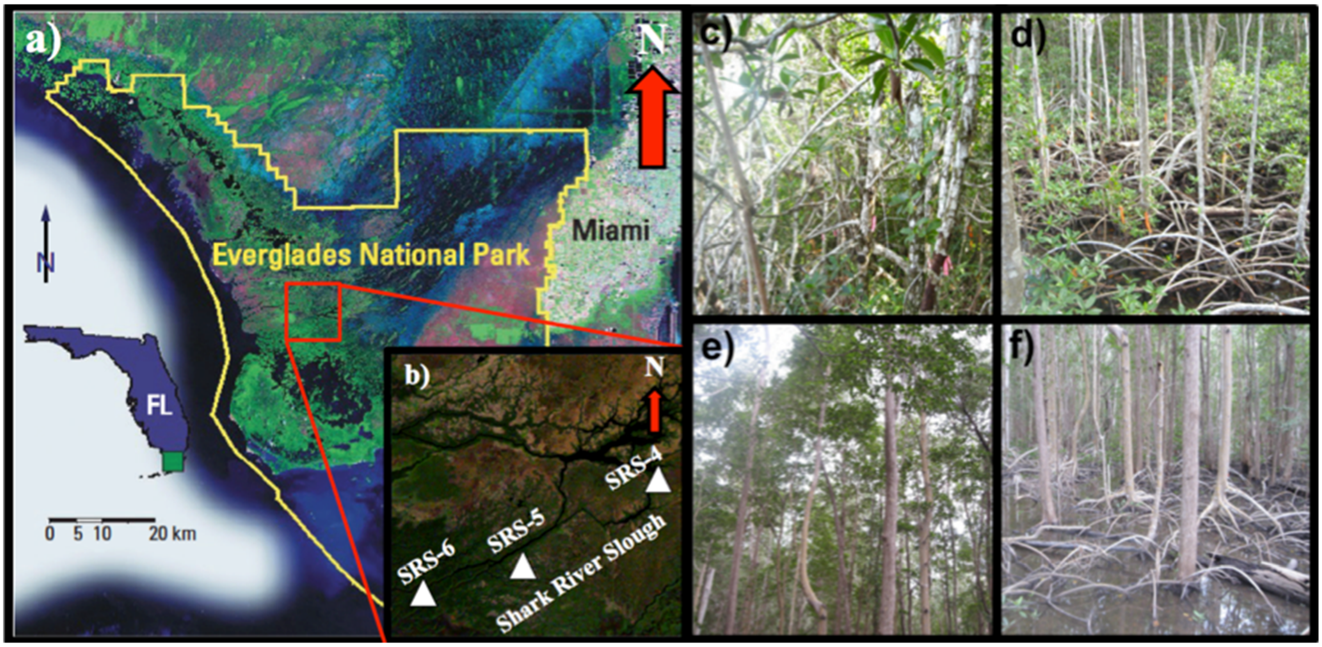

Fig. 1 **a** Location map of the Everglades National Park within the South Florida Peninsula (*USGS TIME Project*). **b** Landsat ETM+image showing a zoom-in view of the study sites along Shark River Slough. **c** Small size mangroves in SRS-4. **d** Intermediate size mangroves in SRS-5. **e** Tall size mangrove canopy in SRS-6. **f** Tall size mangrove prop roots in SRS-6

more evenly distributed and found in SRS-6. Overall, these sites are representative of the spatial distribution of mangrove species and stature in the coastal ENP (Simard et al. 2006).

Methods

Terrestrial Laser Scanner Data Collection

We surveyed the three SRS sites with a TLS between March and April 2011. We used the compact and lightweight Leica ScanStation C10 TLS (Figure S1) because its technical and physical characteristics are suitable for forestry surveys. The Leica TLS complies with and exceeds the minimum requirements suggested for forestry studies (Maas et al. 2008). These requirements are: a minimum data acquisition range of 50 m, a scanning rate of 10,000 points per second for field-time efficiency, an hemispheric field of view for data acquisition flexibility and a spot size of 10 mm to allow for adequate measurements of stem diameter. A summary of the Leica ScanStation C10 technical specifications is provided in Table 1.

At each site, we first delineated a ~50 m by 50 m area of mangroves to sample. Within this area we then placed ~15 identifiable targets and reflectors to aid in the merger of point clouds from individual scans into a single point cloud (Fig. 2). Next, 25 scans (9 in SRS-4, 8 in SRS-5 and 8 in SRS-6) were acquired from various angles to avoid possible occlusions from surrounding vegetation (Fig. 2). Multiple common targets were needed in order to merge the scans (point clouds). After each scan, every target in the field of view was scanned at a higher resolution to precisely identify its center, in order to reduce point cloud merging uncertainty. Finally, hemispherical photos were acquired and automatically assembled using Leica's proprietary software Cyclone v7.4 (Leica 2013), which were useful for bark and tree identification (Fig. 3). The scanning resolution or point spacing for every site was approximately 1 cm at a distance of 10 m. We selected this scanning resolution because it was sufficient to distinguish small vegetation features such as leaves and small branches, and efficient enough to be acquired in approximately 7 min per scan.

Table 1 Leica ScanStation C10 TLS technical specifications

Leica Scanstation C10 TLS Specifications	
Laser Class	3R (eye safe)
Field-of-view	Horizontal (360°) Vertical (270°)
Range	300 m
Scan Resolution	Spot Size (7 mm), Point Spacing (<1 mm)
Scan rate	50,000 points per second
Weight	0.4 kg
Wavelength	Green Laser (532 nm)
Special Features	Integrated Camera, Touch Display

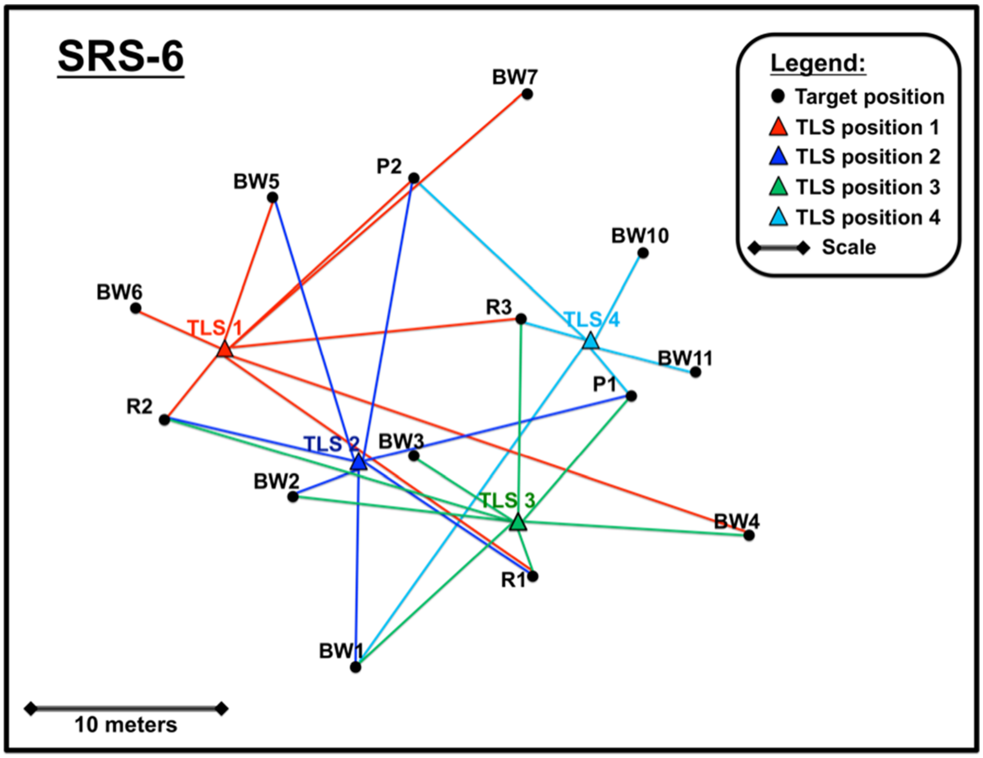

Fig. 2 Map of main target and TLS position network in SRS-6 site. The actual survey included additional targets and scan positions that were omitted from the plot for clarity

TLS Data Processing

The TLS point cloud data were processed using Leica's proprietary software Cyclone v7.4 (Leica 2013). The steps for processing the 3-D point cloud data in Cyclone were: target registration, target registration analysis, and point cloud merging. The target registration step consisted of selecting and merging the targets that were common in every single scan. The target registration analysis consisted of a quality control assessment of the root mean square error (RMS) of the distance between common targets. A low RMS (e.g. 0.08 m) is expected for a registered and merged target. Finally, the various point cloud acquisitions were merged and converted into a single point cloud for each site. Usually, a digital elevation model (DEM) is produced for a TLS study. Due to the extremely flat topography of the ENP a DEM was not necessary for this study.

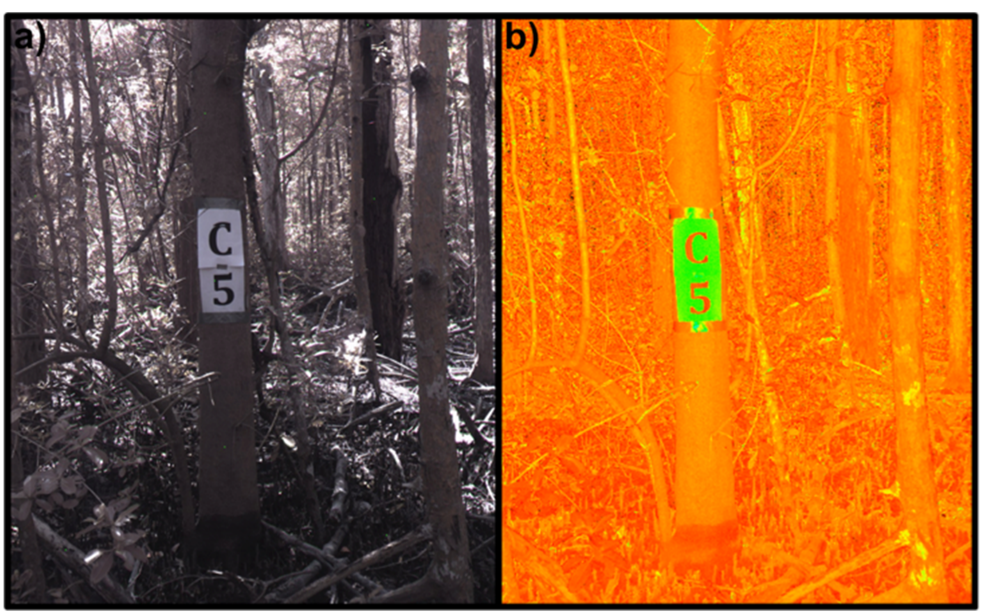

Fig. 3 Lettered tag in an SRS-6 Black mangrove (*Avicennia germinans*). **a** Photograph taken by the TLS. **b** Intensity point cloud acquired by the TLS. Lettered tag visible in the point cloud can be used to help identify a specific mangrove species

TLS Data Post-Processing (Tree Volume Geometry Modelling)

Post-processing or secondary processing after basic data processing (merged point cloud) is an important step towards the use of the point cloud for many applications, including calculating tree volume, which we did in this study. The post-processing of the registered and merged point cloud for each site revealed that mangrove stems could be best modelled as a combination of geometric surfaces called frustums (Fig. 4), as previously suggested by Husch et al. (2002). A frustum is a portion of any geometric solid with the top part severed. However, frustums were not appropriate to model the curved geometry of prop roots. Therefore, we used a combination of two 3-D geometrical solids; toroids and cylinders, in order to model prop roots associated with the Red mangrove species. A toroid or torus is a 3-D doughnut shaped solid, which is created by rotating a circle around curved line (Fig. 5).

Volume and AGB Estimation of Main Stem

Mangrove stem volume estimation was accomplished by modelling the stem as multiple frustums of paraboloids (Fig. 4b). We used the Smalian's formula to estimate the parabolic frustum volume (Husch et al. 2002). The Smalian's formula calculates volume by multiplying the average cross-sectional area of a stem section by the stem section's length. The Smalian's volume is given by:

$$V = (A_T + A_B)/2 * h = \left(\pi {D_T}^2/4 + \pi {D_B}^2/4\right)/2 * h \qquad (1)$$

where V is the volume of the stem section, A_T and A_B are the cross-sectional areas of the upper and bottom sections respectively, h is the length of the stem section and D_T and D_B are the diameters of the upper and bottom sections respectively (Fig. 4c). The first step towards estimating stem volume was dividing the stem into smaller sections (frustums). Using Cyclone software, various cylinders were created at different heights in order to divide the stem into multiple frustums (Fig. 6). The advanced Cyclone software automatically created best-fit cylinders from the point cloud in locations determined by the operator. We defined a frustum as the region between two cylinders. In Cyclone, the two end diameters and the section length were then measured for each frustum. Next, these parameters were incorporated into the Smalian's formula to calculate each frustum volume. Finally, the total stem volume was obtained by summing all of the frustum volumes (Fig. 6).

For *L. racemosa* and *A. germinans* species the main stem was measured from the ground to the first canopy branch in the point cloud. However, for the *R. mangle* species the main stem was measured from the first prop root up to the first canopy branch. We estimated AGB by multiplying our estimated volume by an estimated species-specific WSD. WSD is usually determined by taking wood cores from trees and weighing them before and after oven drying to determine water content. In lieu of doing this, we compiled a list of published WSD measurements of same mangrove species sampled in other neotropicals locations (Saenger 2003; Chave et al. 2009; Zanne et al. 2009; WAC 2013). For each species we estimated the following WSD values and an uncertainty range: 890±33 kg/m^3 for *R. mangle*, 770±42 kg/m^3 for *A. germinans* and

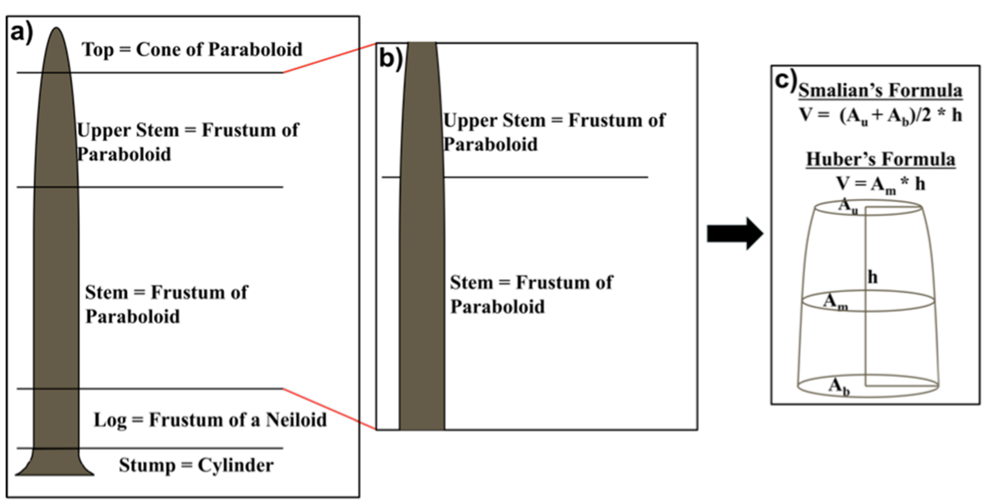

Fig. 4 **a** Suggested frustums by portion of the stem after (Husch et al. 2002). **b** Zoom-in of the frustums used in this study. **c** Frustum of a paraboloid volume

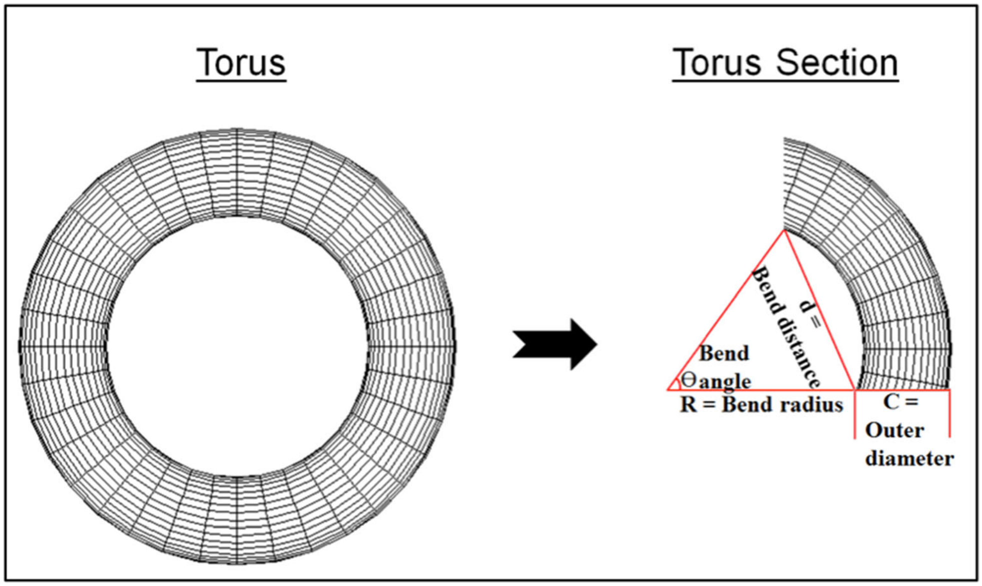

Fig. 5 Toroidal section parameters

620±51 kg/m^3 for *L. racemosa*. A median value was used instead of the average, because the WSD sample size for each species in the previous studies was small and the distributions were not normal.

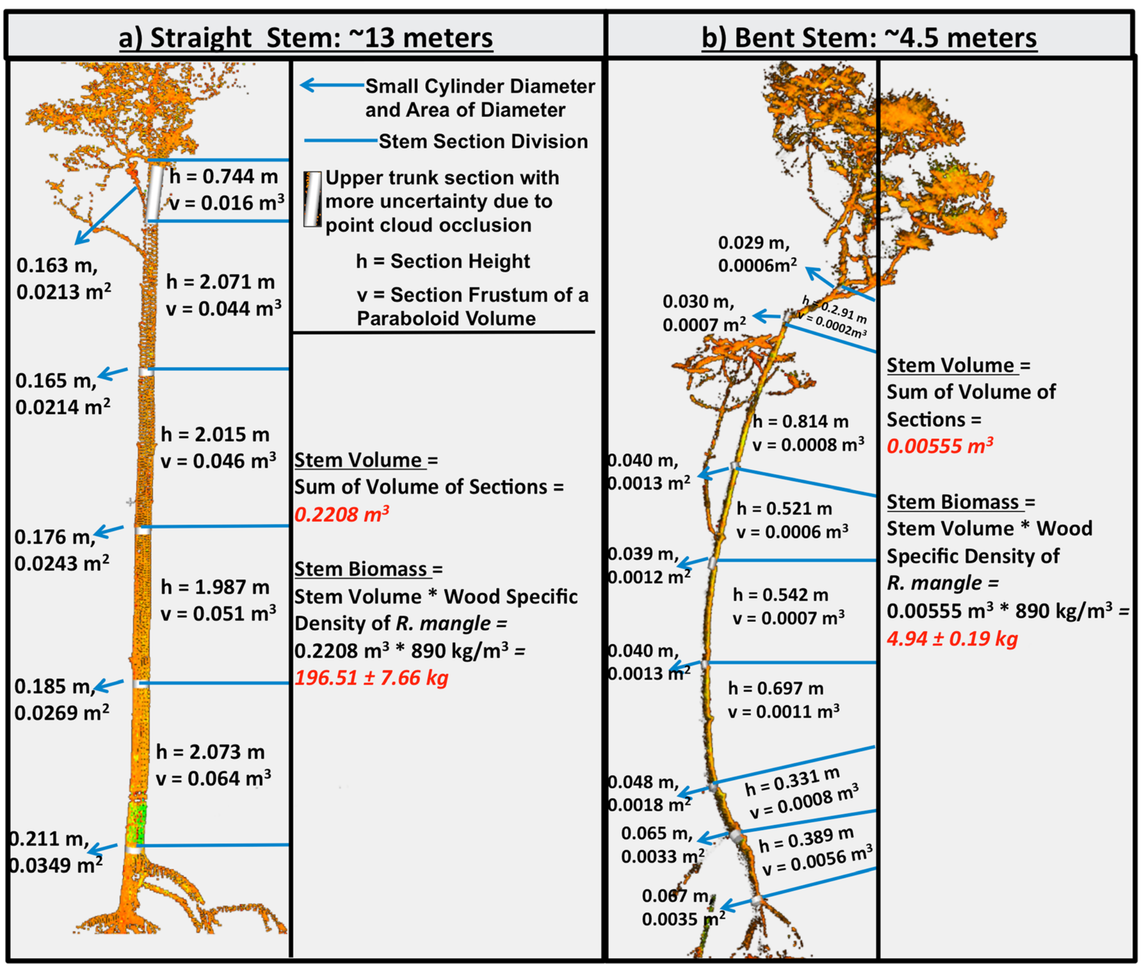

Fig. 6 Volume estimation example for two types of stem shapes. This method is applicable for the three mangrove species. **a** Straight stem volume and AGB estimation. **b** Bent stem volume and AGB estimation. Multiple frustums are required where the stem is bent

Volume and AGB Estimation of Prop Roots (R. mangle)

Prop root volume estimation was accomplished by modelling them as a combination of toroidal sections (Figs. 5 and 7). We used the toric volume formula to estimate the volume of the roots. The toric volume formula is given by:

$$V = \left(\pi^2/4\right) * \left(\left(C+R\right)^2 – R\right)^2\Big) * (C) * (\theta/360); \qquad (2)$$

where C is the outer diameter, R is the bend radius and θ is the bend angle in degrees. For each single prop root, the volume estimation was done in Cyclone (Fig. 7). Although the majority of prop roots resembled toroidal sections, secondary or smaller prop roots mostly located in the SRS-4 and SRS-5 sites, resembled cylinders. The volume of these cylinder-type prop roots was estimated using a simple cylinder volume formula given by:

$$V = \pi R^2 * h; \qquad (3)$$

where R is the radius of the circular cross-section of the cylinder and h is the height of the cylinder.

The volume estimation of the prop roots consisted of the following four steps (Fig. 7). Step 1: Selecting a prop root with sufficient point cloud data. Step 2: Defining a plane that intersects the prop root of interest. Step 3: Rotating the point cloud by 90° and defining a circle that fits the angular bend of the prop root. Step 4: Defining a triangle with three known sides: bend distance, bend radius and adjacent side. We then applied the Law of Cosines to solve the Side-Side-Side (SSS) triangle and estimate the prop root bend angle. Subsequently, we estimated the toric volume with all of the parameters that were acquired from the prop root point cloud. These four steps were repeated for every prop root. Finally, we estimated the total prop root volume by adding each single prop root volume. We estimated the total prop root AGB by multiplying the total prop root volume by the *R. mangle* WSD (890±33 kg/m^3).

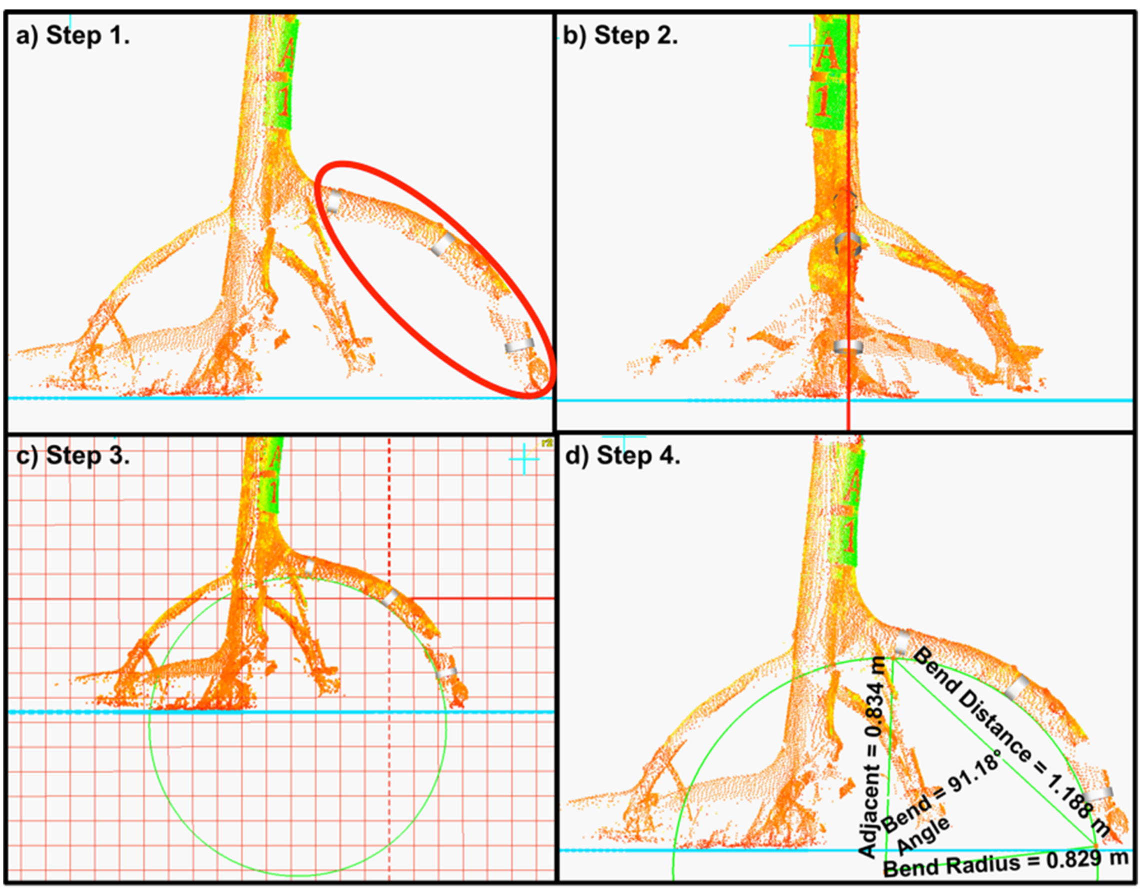

Fig. 7 Root parameters acquisition for using the toric volume estimation technique for a single root: **a** Creation of cylinders to acquire and average prop root diameter in the Y plane. **b** Vertical rotation of the point cloud by 90° to the left and creation of a plane (*blue line*) which cuts the root of interest. This plane is used to create and fit a circle into the root bend. **c** Point cloud rotated 90° to the right. A circle is fitted into the root bend. **d** A triangle with three known sides is created with the circle in order to estimate the root bend angle

Canopy Correction

The canopy structure and tree height were not accurately acquired by our TLS survey, because (1) the top sections of canopies cannot be imaged from the ground, and (2) there were line-of-sight obstructions between the TLS and the canopies. In order to be able to compare our results with published mangrove allometry, a canopy estimate was needed. Mangrove canopy AGB allocation estimates range approximately from 10 to 30 % of the total AGB (Clough et al. 1997; Fromard et al. 1998; Komiyama et al. 2005). For this reason we applied a canopy correction (20±10 %) to our TLS-based AGB results. We thus multiplied our estimated TLS-based AGB (stem+prop roots) by 1.25 yielding a canopy allocation of 20 % of the total AGB every single tree. As a real example from a mangrove in SRS-5, we obtained a TLS-based estimate (stem+prop roots) of 200.2 kg for a specific tree. Multiplying its AGB by a factor of 1.25 would give a total AGB estimate of 250.2. Thus, in this case, the canopy AGB estimate would be 50 kg, which represents 20 % of the total AGB. The±10 % canopy biomass uncertainty was included in the total uncertainty calculation for every tree. We applied our suggested canopy correction (1.25) to every processed mangrove.

Mangrove Allometry from TLS Data

In order to create allometric equations for their use on ENP mangroves, we generated two regressions based on our TLS results (Fig. 8) with the goal of developing allometric equations common to all mangrove species, as well as developing an equation for *R. mangle* which is the most abundant species. Our allometric equations are based on fitting our data using a power function equation. White and Gould (1965) proposed and demonstrated that the power equation has a relationship with allometry. The power relationship is given by:

$$F(x) = a * x^b; \tag{4}$$

where $F(x)$ or y is AGB, x is DBH, a represents the allometry coefficient and b represents the proportionality between cumulated variables.

Mangrove Allometry Comparison

In order to test the reliability of the TLS-based AGB estimations, we compared our results with published mangrove allometric equations. As there are no published allometry for the SRS ENP sites, we used tropical mangrove allometric equations that estimate AGB from DBH (Imbert and Rollet 1989; Fromard et al. 1998), to compare with our AGB results. We also used the allometric equations from Smith and Whelan (2006), which were developed for three different ENP sites (Black Forest: ~27 km from SRS, Mud Bay: ~13 km from SRS and Highland Beach: ~20 km from SRS). These published studies include site-specific allometric equations for the three mangrove species studied in this investigation and use DBH as an AGB predictor. Additionally, we compared our TLS-based AGB results with the mangrove common equation established by Chave et al. (2005), which uses DBH and WSD to estimate AGB and can be applied to any mangrove species. We used DBH measurements acquired from our TLS dataset as input for the various allometric equations. Tables S1 (SRS-4), S2 (SRS-5) and 3 (SRS-6) present the comparison between

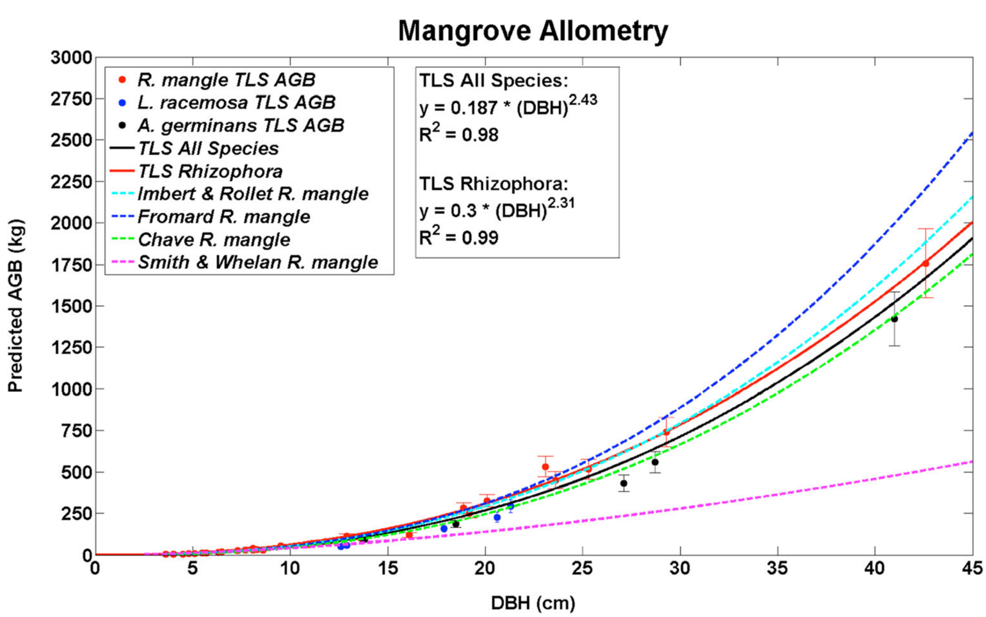

Fig. 8 Mangrove allometry between DBH and AGB. Data points with uncertainty are derived from our TLS estimates. The regressions calculated in this study are shown in black and red solid lines and published regressions (Imbert and Rollet 1989; Fromard et al. 1998; Chave et al. 2005; Smith and Whelan 2006) are shown for comparison purposes

our TLS-based AGB estimations and those estimated from published allometric equations.

Uncertainty Analysis

Our AGB estimates were calculated by multiplying the TLS-derived tree volume by WSD and then correcting for the unobserved canopy. The calculation components (volume, WSD, and canopy corrections) are known with a range of uncertainties. In order to evaluate the combined contribution of the uncertainties on the AGB estimates, we used an uncertainty propagation analysis. Sources of uncertainties are: TLS measurement error, geometrical parameters (Table 2) of the stem volume (eq. 1) and prop root volume (eq. 2), WSD, and the canopy correction.

Parameter Uncertainties

TLS Measurement Errors The point spacing or resolution of the TLS was set to 1 cm per 10 m, which has an uncertainty of 0.01 divided by √3 (standard uncertainty for a digital device); the resulting uncertainty in very small (~0.5 %). As TLS is a high precision tool, point spacing or resolution resulted in a very small uncertainty, which is negligible with respect to the other parameter uncertainties and, hence, omitted from the calculations.

Geometrical Parameters Repeatedly estimating the geometric parameters provides a measure of repeatability and uncertainty (Tables S3, S4). As an example, the fitting of cylinders for the acquisition of diameter measurements into the point cloud was essential in order to estimate the paraboloidal volume of the mangrove stems (Table S3) and toroidal volume of prop roots (Table S4). The repeated diameter fit analysis revealed the following uncertainties: 0.51–1.32 %, depending on vertical location of the cylinder along the stem with an average stem uncertainty of 0.84 %. We conducted the same repeatability uncertainty analysis for every parameter involved in the volumetric calculations. For the frustum of paraboloidal/stem volume parameters (Table S3), the uncertainties were: 0.84 % for the diameter (average stem diameter uncertainty) and 0.65 % for the paraboloid's height (Table 2). For the toroidal/prop root volume parameters (Table S4) the uncertainties were: 2.0 % for the prop root outer diameter, 0.96 % for the bend radius and 1.5 % for the bend angle (Table 2).

Wood Specific Density For each species we estimated, based on literature values (section 3.3.1), the following median WSD value and an uncertainty range: 890±3.7 % kg/m^3 for *R. mangle*, 770±5.5 % kg/m^3 for *A. germinans* and 620±8.2 % kg/m^3 for *L. racemosa* (Table 2).

Canopy Correction A canopy correction with an uncertainty of 10 % (Section 3.4) was applied to the AGB estimations as the TLS in not able to acquire the entire canopy structure.

Estimation of Uncertainty Propagation

Our uncertainty propagation analysis approach is based on our method for estimating total AGB. For *L. racemosa* and *A. germinans*, AGB is defined as:

$$AGB_{Total} = AGB_{stem} + AGB_{canopy}; \tag{5}$$

where AGB_{stem} is stems's AGB calculated as a product of the paraboloidal volume (1) and WSD and AGB_{canopy} is the canopy correction. For *R. mangle*, the total AGB is defined as:

$$AGB_{Total} = AGB_{proproot} + AGB_{stem} + AGB_{canopy}; \tag{6}$$

where the additional $AGB_{proproot}$ is a product of the toroidal volume (2) and WSD

The stem AGB (AGB_{stem}) for the three species and prop root AGB ($AGB_{proproot}$) for *R. mangle* are product of several volumetric parameters (Tables S3 and S4) and WSD. Calculating the uncertainty for a frustum of a paraboloid can be complicated, as the volume equation contains both multiplication and addition products (1). However, we can simplify the calculations by assuming that both diameters are identical ($D_T \approx D_B$) and calculate the uncertainty of a cylinder. In this case the stem biomass uncertainty ratio is found by applying the multiplication uncertainty propagation equation (Taylor 1997), which for a cylinder is:

$$\frac{\delta AGB_{stem}}{|AGB_{stem}|} = \sqrt{2\left(\frac{\delta D}{D}\right)^2 + \left(\frac{\delta H}{H}\right)^2 + \left(\frac{\delta WSD}{WSD}\right)^2} \tag{7}$$

where $\frac{\delta D}{D}$, $\frac{\delta H}{H}$ and $\frac{\delta WSD}{WSD}$ represent the uncertainty ratio of the diameter, height and WSD respectively.

Similarly, uncertainty propagation for the toroidal volume calculations (2) was estimated by assuming that the prop root's outer diameter is much smaller than the prop root radius (C<< R). This assumption reduces the prop root uncertainty AGB ratio calculations to:

$$\frac{\delta AGB_{proproot}}{|AGB_{proproot}|} = \sqrt{2\left(\frac{\delta C}{C}\right)^2 + \left(\frac{\delta R}{R}\right)^2 + \left(\frac{\delta \theta}{\theta}\right)^2} \tag{8}$$

where $\frac{\delta C}{C}$, $\frac{\delta R}{R}$ and $\frac{\delta \theta}{\theta}$ represent the uncertainty ratio of the outer diameter, the bend radius and the bend angle, respectively.

Table 2 Parameter uncertainty estimates for the three mangrove species in the ENP

Mangrove AGB Segment	Parameter	Uncertainty (%)	Uncertainty Propagation (%) Eq. (7) for Stem, Eq. (8) for Prop Root
L. racemosa AGB_{stem}	Height (*H*)	0.65	8.3
	Diameter (*D*)	0.84	
	WSD	8.2	
A. germinans AGB_{stem}	Height (*H*)	0.65	5.7
	Diameter (*D*)	0.84	
	WSD	5.6	
R. mangle AGB_{stem}	Height (*H*)	0.65	3.9
	Diameter (*D*)	0.84	
	WSD	3.7	
R. mangle $AGB_{proproot}$	Outer Diameter (*C*)	2.0	5.0
	Bend Radius (*R*)	0.96	
	Bend Angle (°)	1.5	
	WSD	3.7	

Results

AGB Estimation and Allocation

Our results included 40 processed mangroves (10 *R. mangle* per site, 5 *L. racemosa* in SRS-6 and 5 *A. germinans* in SRS-6). Examples of our TLS- based mangrove stem volume estimations along with AGB results are presented in Table 3 for a sub-sample (3 from each site) of *R. mangle* individuals. The rest of the results are provided in Tables S1 and S2 of the Supplementary Material. Our calculations of the stem AGB ranged between 2.68±0.1 kg in an SRS-4 small mangrove up to 1295.35±50.52 kg in a tall mangrove located in SRS-6 (Table 3). Another objective of this study was estimating prop root volume and AGB. Table 3 also shows examples of total prop root volume and AGB estimations for the same sub-sample (3 from each site) of *R. mangle* individuals. Prop root AGB ranged from 0.47±0.02 kg in a small mangrove located at SRS-4 up to 109.87±5.5 kg in a tall mangrove located at SRS-6 (Table 3). Canopy AGB estimations from the proposed canopy correction explained in section 3.4 are presented in Table 3 for this sub-sample.

Accounting for prop root, stem and canopy AGB, our TLS-based results for the SRS sites were in the AGB range of 3.9±0.4 to 31.3±3.4 kg per tree in the short mangrove site (Table S1), 27.4±3.0 to 119.1±12.9 kg per tree in the intermediate site (Table S2) and 52.1±6.7 to 1756.5±189.7 kg per tree in the tall mangrove site

Table 3 Mangrove stem/prop root volume, stem/prop root AGB and canopy AGB estimations for a sub-sample of 9 of the 30 processed *Rhizophora mangle* trees (WSD=890±33 kg/m^3)

Site	TLS-based Main Stem Volume (m^3)	Main Stem AGB (kg)	TLS-based Prop Root Volume (m^3)	Prop Root AGB (kg)	Canopy AGB from Canopy Correction (kg)
SRS-4	0.00301	2.68±0.10	0.000528	0.47±0.02	0.79±0.08
	0.00555	4.94±0.19	0.000640	0.57±0.03	1.38±0.14
	0.00864	7.69±0.30	0.001888	1.68±0.08	2.34±0.23
SRS-5	0.07634	67.98±2.65	0.01417	12.62±0.06	20.15±2.06
	0.07304	65.01±2.54	0.02269	20.19±1.01	21.30±2.13
	0.09016	80.24±3.13	0.01687	15.01±0.75	23.81±2.38
SRS-6	0.22080	196.51±7.66	0.03140	27.96±1.40	56.12±5.6
	0.41680	370.95±14.47	0.06187	55.06±2.75	106.50±10.70
	1.45400	1295.35±50.52	0.12340	109.87±5.50	351.31±35.13

(Table 4). AGB allocation results were estimated by comparing the proportion of prop root, stem and estimated canopy AGB in the 30 *R. mangle* individuals (10 per site). Overall, prop root allocation ranged from 10 to 20 %, stem allocation was in the range of 60–70 %, and based on literature's values, canopy allocation was estimated in the range of 10–30 %. Comparing the AGB allocation among the sites did not yield systematics trends.

AGB Uncertainty

The total AGB uncertainty (δAGB_{Total}) for the three species was calculated as the summation of the individual uncertainties of the mangrove segments. Thus, we used the addition uncertainty propagation equation (Taylor 1997). In our study, it is defined as:

$$\delta AGB_{Total} = \sqrt{\left(\delta AGB_{stem}\right)^2 + \left(\delta AGB_{proproot}\right)^2 + \left(\delta AGB_{canopy}\right)^2} \qquad (9)$$

where δAGB_{stem}, $\delta AGB_{proproot}$ and δAGB_{canopy} represent the uncertainty values (in kilograms) of AGB_{stem}, $AGB_{proproot}$ *(R.mangle)*, and AGB_{canopy}, respectively. In order to use the uncertainty ratio, values were calculated in equations (7) and (8), we then scaled them by multiplying them with the calculated AGB for each tree. This scaling is accurate for the *L. racemosa* and *A. germinans*. However, for *R. mangle* the scaling was conducted, for simplicity, using one third of AGB_{stem}, because the ratio of $AGB_{proproot}/AGB_{stem}$ was smaller than a third (Table 5). The total AGB uncertainty for each species was calculated using (eq. 9), which revealed the following uncertainties: 10.8 % for *R. mangle*, 12.9 % for *L. racemosa* and 11.5 % for *A. germinans* (Table 5).

Mangrove Allometry from TLS Data

We created two regressions with our TLS-based results (Fig. 8) in order to generate allometric equations for their use on ENP mangroves. Our estimated individual AGB values versus DBH measurements, along with our TLS-based regressions are shown in Fig. 8. For comparison, the regressions from the previous allometric studies were also plotted. The goal of our regressions was to develop a common allometric equation (all data points from the three species) and the creation of a *R. mangle* allometric equation, which is the most abundant species. Our *R. mangle* regression ($AGB=0.3 * x^{2.31}$) is more similar to the Imbert and Rollet (1989) regression (Fig. 8). Our proposed common (three species) mangrove regression ($AGB=0.187 * x^{2.43}$) resembles that of Chave et al. (2005), which is also a common mangrove regression. Overall, our SRS-4, SRS-5 and SRS-6 AGB

Table 4 SRS–6 TLS-based mangrove AGB compared with published mangrove allometry (10 *Rhizophora mangle* - WSG=890±33 kg/m^3, 5 *Laguncuria racemosa* - WSG=620±51 kg/m^3, 5 *Avicennia germinans* - WSG=770±42 kg/m^3)

Mangrove Species	TLS-based DBH (cm)	TLS-based AGB (kg); with Canopy Correction	AGB (kg); (Imbert and Rollet 1989)	AGB (kg); (Fromard et al. 1998)	AGB (kg); (Chave et al. 2005)	AGB (kg); (Smith and Whelan 2006)
R. mangle	11.0	61.20±6.61	66.48	65.29	55.84	49.05
	12.9	112.21±12.12	98.53	98.80	82.77	64.63
	18.9	280.60±30.30	253.09	266.69	212.60	125.19
	19.2	250.20±27.02	263.13	277.84	221.03	128.65
	20.1	326.61±35.27	294.66	312.98	247.51	139.26
	23.1	532.51±57.51	415.47	449.37	349.0	177.18
	23.6	450.86±48.69	438.04	475.10	367.95	183.87
	25.3	517.48±55.89	520.15	569.28	436.93	207.40
	29.3	740.63±80.00	747.45	833.81	627.86	267.39
	42.6	1756.53±189.71	1883.92	2206.35	1582.49	511.10
L. racemosa	12.6	52.08±6.72	60.95	57.48	66.60	48.16
	12.9	58.34±7.53	64.25	60.96	70.58	50.40
	17.9	156.55±20.19	133.82	138.27	158.53	94.84
	20.6	227.09±29.29	183.32	196.46	224.29	124.38
	21.3	293.29±37.83	197.57	213.57	243.58	132.67
A. germinans	13.8	95.38±10.97	74.02	76.18	95.35	64.50
	18.5	187.55±21.57	155.84	153.94	196.67	113.69
	27.1	432.45±49.73	410.95	384.82	504.97	237.88
	28.7	560.0±64.40	475.41	441.62	581.83	265.79
	41.0	1421.55±163.48	1176.31	1039.46	1404.12	529.81

Table 5 Total AGB uncertainty estimates (%) for the three mangrove species in the ENP

Total AGB Uncertainty (%) for Each Species using Eq. (9)			
Mangrove Species	Mangrove AGB Segment Uncertainty (%)		Total AGB Uncertainty (%)
L. racemosa	AGB_{stem}	8.3	12.9
	AGB_{canopy}	10	
A. germinans	AGB_{stem}	5.6	11.5
	AGB_{canopy}	10	
R. mangle	AGB_{stem}	3.9	10.8
	$AGB_{proproot}$	1.3*	
	AGB_{canopy}	10	

*For *R. mangle* the scaling of in Eq. (8) is conducted, for simplicity, using one third of AGB_{stem}, because the ratio of $AGB_{proproot}/AGB_{stem}$ is smaller than a third (Table 3)

results were inside or close to the range of the estimations obtained from the three published allometric studies, suggesting the potential of TLS as an AGB estimation tool. A trend of stem height and AGB was noticed in our study; however, as the focus of the paper was to compare allometry of published studies that predict AGB from DBH this information was not included.

Discussion

Mangrove Allometry Comparison

A visual comparison between our results and the published mangrove allometry in the form of regressions is presented in Fig. 8. Below 20 cm DBH, our data agree with all of the *R. mangle* regressions except Smith and Whelan (2006). Above 20 cm, our data agree with the Imbert and Rollet (1989) and Chave et al. (2005) regressions, but not with the regression of Fromard et al. (1998). The misfit with Fromard's regression above 20 cm could be due to the fact that it was created for a limited DBH range (up to 32 cm for *R. mangle*). Our results best agree with Imbert and Rollet's regression. Interestingly, the ENP study by Smith and Whelan (2006) predicts lower AGB values when compared to all of the regressions. However, as their study suggested, environmental factors such as the hydrology, salinity, nutrient availability of a specific region or site could yield different and variable AGB values. Although not presented in Fig. 8 as regressions (not enough points), our *L. racemosa* and *A. germinans* mangrove results (Table 3) were highly comparable to the common equation developed by Chave et al. (2005). This resemblance could be due to the fact that the common equation uses WSD in addition to DBH (up to 50 cm) to constrain the AGB estimation. However, the *L. racemosa* and *A. germinans* equations developed by Fromard et al. (1998) and Imbert and Rollet (1989) use only DBH for a more limited range and indicated less agreement when compared to our estimates and the Chave et al. (2005) estimations. Although we extrapolated predicted values from the published studies (Fig. 8) for comparison purposes, it is of upmost importance to understand that using DBHs larger than those specified by the allometric equations might give more AGB uncertainties. Furthermore, site-specific variations in mangrove architecture between our study areas and those published, including the ENP study by Smith and Whelan (2006) could also yield AGB differences.

TLS Data Analysis

In our TLS data analysis, for fairly straight stems (Fig. 6a) we found that the creation of four frustum sections best approximated the true volume of the stem, as the creation of more sections did not change the estimated volume by a significant quantity. This was the case for most of the stems of the more mature mangroves located in SRS-6, which can reach up to ~23 m in canopy height. We suggest that this method is applicable for the three species in the ENP. On the other hand, special consideration had to be taken to estimate the volume of bent stems (Fig. 6b). The 3-D point cloud showed that small to intermediate size mangroves (up to ~13 m) located in SRS-4 and SRS-5 tended to have a more bent stem structure. Our approach for the volume calculation of a bent stem consisted of starting with a frustum section at approximately every bending point in order to create smaller straight stem sections (Fig. 6b). For prop roots, whether they resemble toroidal sections or cylinders, we estimated the total prop root volume of a particular tree as the sum of every singular prop root volume (Fig. 7).

Our methodology and analysis was focused on the AGB estimation of the main stem and prop roots as a substantial amount of the above-ground carbon is stored in these areas. It is important to understand AGB allocation in these two structures, as they are the foundation of biomass replacement for branches, leaves and twigs which are shed and converted to litterfall (detritus and deadwood) throughout the year (Clough

1992). Although our prop root and stem TLS-based AGB allocation estimations are comparable with published mangrove studies (Clough et al. 1997), biogeographic dissimilarities and site-specific environmental factors could result in different AGB values and allocation for different regions (Smith and Whelan 2006).

Conclusion

We used TLS data to estimate mangrove stem and prop root volume and AGB in various mangrove individuals located in the ENP. The use of TLS data in addition to the proposed canopy correction proved to be successful in estimating mangrove AGB and showed comparable results with published mangrove allometry. We suggest that the methodology presented in this paper could be nearly as accurate as destructive techniques, as tree volume is analyzed and processed as a tree-by-tree basis with a state-of-the-art tool. TLS data presents a unique opportunity to evaluate and analyze prop root AGB and structure, which has not been done in much detail. In addition, TLS presents the advantage of acquiring and analyzing tall mangroves, which is not possible with traditional methods, as it would encompass an enormous task to harvest and sample such mangroves. Furthermore, mangrove harvesting is prohibited in protected ecosystems such as the ENP. The results of this case study revealed that although mangrove structure could be complex (bent structures) there is potential for the use of TLS in this kind of wetland environment.

We suggest that the use of TLS could be a substitute tool to destructive sampling and harvesting, towards the creation of allometric equations. For this reason we proposed ENP mangrove allometric equations with the data acquired and analyzed in this study. Sources of discrepancies between our estimations and the published allometry may have arisen from uncertainty or from the allometric equations themselves, which were developed for specific mangrove forest locations. Future research should seek the integration of Airborne LiDAR data with TLS data in order to acquire the full canopy structure, enhance the total AGB estimation and expand the study area. The use of TLS presents the advantage of estimating various sources of uncertainties, which is not common for this type of study. It is of upmost importance to mention that our TLS methodology is not limited to AGB studies. There is potential to apply these methods to quantify structural damage after storms, hurricanes and fires, or to monitor stand development along different sites. This is the first reported TLS study for a mangrove ecosystem.

Acknowledgments We thank the associate editor and two anonymous reviewers for very constructive comments and suggestions. We also thank the Everglades National Park for enabling us to conduct the study within the protected area of the park. The material on this study was based upon work supported by the National Science Foundation Graduate Research Fellowship Program under Grant No. DG1E-0951782 and by NASA Cooperative Agreement No. NNX10AQ13A (WaterSCAPES: Science of Coupled Aquatic Processes in Ecosystems from Space). This material was developed in collaboration with the Florida Coastal Everglades Long-Term Ecological Research program under National Science Foundation Grant No. DEB-1237517.

References

Alongi DM (2002) Present state and future of the world's mangrove forests. Environmental Conservation 29(03):331–349

Alongi DM (2012) Carbon sequestration in mangrove forests. Carbon Management 3(3):313–322

Barr JG, Fuentes JD, Engel V, Zieman JC (2009) Physiological responses of red mangroves to the climate in the Florida Everglades. Journal of Geophysical Research – Biogeosciences 114

Castaneda-Moya E, Twilley RR, Rivera-Monroy VH, Marx BD, Coronado-Molina C, Ewe SML (2011) Patterns of root dynamics in mangrove forests along environmental gradients in the Florida coastal Everglades, USA. Ecosystems 14(7):1178–1195

Chave J, Andalo C, Brown S, Cairns MA, Chambers JQ, Eamus D, Folster H, Fromard F, Higuchi N, Kira T, Lescure JP, Nelson BW, Ogawa H, Puig H, Riera B, Yamakura T (2005) Tree allometry and improved estimation of carbon stocks and balance in tropical forests. Oecologia 145(1):87–99

Chave J, Coomes D, Jansen S, Lewis SL, Swenson NG, Zanne AE (2009) Towards a worldwide wood economics spectrum. Ecology Letters 12(4):351–366

Clawges R, Vierling L, Calhoon M, Toomey M (2007) Use of a ground-based scanning lidar for estimation of biophysical properties of western larch (Larix occidentalis). International Journal of Remote Sensing 28(19):4331–4344

Clough BF (1992) Primary productivity and growth of mangrove forests, Tropical mangrove ecosystems. Coastal and Estuarine Studies. AGU Washington, DC, pp 225–249.

Clough BF, Dixon P, Dalhaus O (1997) Allometric relationships for estimating biomass in multi-stemmed mangrove trees. Australian Journal of Botany 45(6):1023–1031

Coronado-Molina C, Day JW, Reyes E, Perez BC (2004) Standing crop and aboveground biomass partitioning of a dwarf mangrove forest in Taylor River Slough, Florida. Wetlands Ecology and Management 12(3):157–164

Donato DC, Kauffman JB, Murdiyarso D, Kurnianto S, Stidham M, Kanninen M (2011) Mangroves among the most carbon-rich forests in the tropics. Nature Geoscience 4(5):293–297

Fromard F, Puig H, Mougin E, Marty G, Betoulle JL, Cadamuro L (1998) Structure, above-ground biomass and dynamics of mangrove ecosystems: new data from French Guiana. Oecologia 115(1-2):39–53

Giri C, Ochieng E, Tieszen LL, Zhu Z, Singh A, Loveland T, Masek J, Duke N (2011) Status and distribution of mangrove forests of the world using earth observation satellite data. Global Ecology and Biogeography 20(1):154–159

Gong WK, Ong JE (1990) Plant biomass and nutrient flux in a managed mangrove forest in Malaysia. Estuarine, Coastal and Shelf Science 31(5):519–530

Hopkinson C, Chasmer L, Young-Pow C, Treitz P (2004) Assessing forest metrics with a ground-based scanning lidar. Canadian Journal of Forest Research 34(3):573–583

Husch B, Beers TW, Kershaw Jr JA (2002) Forest mensuration. Wiley.

Imbert D, Rollet B (1989) Phytmassaerienne et production primaire dans la mangrove du Grand Cul-de-sac Marine (Guadeloupe, Antilles francaises). Bulletin D Ecologie 20:27–39

Jennerjahn TC, Ittekkot V (2002) Relevance of mangroves for the production and deposition of organic matter along tropical continental margins. Naturwissenschaften 89(1):23–30

Kauffman JB, Heider C, Cole TG, Dwire KA, Donato DC (2011) Ecosystem carbon stocks of Micronesian mangrove forests. Wetlands 31(2):343–352

Komiyama A, Poungparn S, Kato S (2005) Common allometric equations for estimating the tree weight of mangroves. Journal of Tropical Ecology 21:471–477

Komiyama A, Ong JE, Poungparn S (2008) Allometry, biomass, and productivity of mangrove forests: a review. Aquatic Botany 89(2): 128–137

Leica (2013) Cyclone 3D Point Cloud Processing Software. Last accessed: July 2013. From: http://hds.leica-geosystems.com/en/Leica-Cyclone_6515.htm

Liang XL, Litkey P, Hyyppa J, Kaartinen H, Vastaranta M, Holopainen M (2012) Automatic stem mapping using single-scan terrestrial laser scanning. IEEE Transactions on Geoscience and Remote Sensing 50(2):661–670

Lugo AE, Snedaker SC (1974) The ecology of mangroves. Annual Review of Ecology and Systematics 5(1):39–64

Maas H-G, Bienert A, Scheller S, Keane E (2008) Automatic forest inventory parameter determination from terrestrial laser scanner data. International Journal of Remote Sensing 29(5): 1579–1593

Mcleod E, Chmura GL, Bouillon S, Salm R, Björk M, Duarte CM, Lovelock CE, Schlesinger WH, Silliman BR (2011) A blueprint for blue carbon: toward an improved understanding of the role of vegetated coastal habitats in sequestering CO2. Frontiers in Ecology and the Environment 9(10):552–560

Rivera-Monroy VH, de Mutsert K, Twilley RR, Castaneda-Moya E, Romigh MM, Davis SE (2007) Patterns of nutrient exchange in a riverine mangrove forest in the Shark River Estuary, Florida, USA. Hidrobiologica 17(2):169–178

Rivera-Monroy VH, Castañeda-Moya E, Barr JG, Engel V, Fuentes JD, Troxler TG, Twilley RR, Bouillon S, Smith TJ, O'Halloran TL (2013) Current methods to evaluate net primary production and carbon budgets in mangrove forests. Methods in Biogeochemistry of Wetlands (methodsinbiogeo):243–288.

Ross M, Ruiz P, Telesnicki G, Meeder J (2001) Estimating above-ground biomass and production in mangrove communities of Biscayne National Park, Florida (U.S.A.). Wetlands Ecology and Management 9(1):27–37

Saenger P (1982) Morphological, anatomical and reproductive adaptations of Australian mangroves. In: B.F. Clough, mangroves ecosystems in Australia. Australia National University Press, Canberra, pp 153–191

Saenger P (2003) Mangrove ecology, silviculture and conservation. Springer SBM.

Sánchez BG (2005) Belowground productivity of mangrove forests in southwest Florida, Faculty of Louisiana State University and Agricultural and Mechanical College in partial fulfillment of the requirements for the degree of Doctor of Philosophy in The Department of Oceanography and Coastal Sciences by Beatriz Giraldo Sánchez BS, Universidad Del Valle.

Schlesinger WH, Bernhardt ES (2013) Biogeochemistry: An analysis of global change 3th Edition. Access Online via Elsevier, 2013.

Seidel D, Beyer F, Hertel D, Fleck S, Leuschner C (2011) 3D-laser scanning: A non-destructive method for studying above- ground biomass and growth of juvenile trees. Agricultural and Forest Meteorology 151(10):1305–1311

Simard M, Zhang K, Rivera-Monroy VH, Ross MS, Ruiz PL, Castañeda-Moya E, Twilley RR, Rodriguez E (2006) Mapping height and biomass of mangrove forests in everglades national park with SRTM elevation data. Photogrammetric Engineering and Remote Sensing 72(3):299–311

Smith TJ III, Whelan KRT (2006) Development of allometric relations for three mangrove species in south Florida for use in the greater everglades ecosystem restoration. Wetlands Ecology and Management 14(5):409–419

Tansey K, Selmes N, Anstee A, Tate NJ, Denniss A (2009) Estimating tree and stand variables in a Corsican Pine woodland from terrestrial laser scanner data. International Journal of Remote Sensing 30(19): 5195–5209

Taylor JR (1997) An introduction to error analysis: The study of uncertainties in physical measurements. University Science Books.

Twilley R, Chen R, Hargis T (1992) Carbon sinks in mangroves and their implications to carbon budget of tropical coastal ecosystems. Water, Air, and Soil Pollution 64(1-2):265–288

WAC (2013) World of Agroforestry Centre - Wood Density Database. Last accessed: July 2013. From: http://worldagroforestry.org/sea/products/afdbases/wd

Watt PJ, Donoghue DNM (2005) Measuring forest structure with terrestrial laser scanning. International Journal of Remote Sensing 26(7): 1437–1446

White JF, Gould SJ (1965) Interpretation of the coefficient in the allometric equation. American Naturalist 99(904):5–18

Zanne AE, Lopez-Gonzalez G, Coomes DA, Ilic J, Jansen S, Lewis SL, Miller RB, Swenson NG, Wiemann MC, Chave J (2009) Data from: Towards a worldwide wood economics spectrum. Dryad data repository